

Editorial Manager(tm) for Journal of Computational Neuroscience
Manuscript Draft

Manuscript Number:

Title: On the effect of fixational eye movements on the expression of retinal ganglion cell nonlinearities

Article Type: Regular Article

Section/Category:

Keywords: Motion Perception; Eye Movements; Fixation; Model; Retina;
Nonlinearities; Magnocellular Pathway

Corresponding Author: Dr. Matthias Helge Hennig, PhD

Corresponding Author's Institution: University of Edinburgh

First Author: Matthias Helge Hennig, PhD

Order of Authors: Matthias Helge Hennig, PhD; Florentin Wörgötter, PhD

Manuscript Region of Origin:

Abstract: Psychophysical evidence suggests that during fixation involuntary eye movements can lead to powerful illusions of apparent motion and other instabilities. In this work, we used a detailed biophysical model of the mammalian retina to investigate potential effects of fixational eye movements on retinal ganglion cell activity during fixation of a star-shaped stimulus. The model simulates the population activity of linear, sustained (parvocellular) and nonlinear, transient (MC) ganglion cell type, and we investigated the spatio-temporal activity patterns of these cell types. We found two very distinct effects: a fading of complete wedges of the star and an apparent splitting of stimulus lines. These effects only occur in the MC-cell population and resemble the perceived instabilities during fixation of a star-shaped or related stimuli. The analysis of simulated single cell activity shows that fading effect is caused by an expression of the aperture problem in retinal ganglion cells, and the splitting effect is a result of spatio-temporal nonlinearities in MC-cells. We therefore propose that certain illusory percepts may be traced back to specific properties of retinal ganglion cell responses.

Dear Editor,

please find enclosed our manuscript "On the effect of fixational eye movements on the expression of retinal ganglion cell nonlinearities", which we would like to submit for consideration for publication in the Journal of Computational Neuroscience. The final version of the manuscript has been seen and agreed upon by both authors.

Using a rather detailed model of the vertebrate retina, the paper addresses effects of fixational eye movements (microtremor and drift) on retinal ganglion cell responses. In particular, we investigated a stimulus known to elicit visual illusions to assess how nonlinearities in ganglion cell receptive fields may affect the resulting visual percept. On the basis of our modelling results, we derive several experimentally testable predictions. In summary, here we attempt to link high-level visual perception to specific physiological properties of individual neurons, and we believe this approach may be of interest to the computational neuroscience community.

Please note that two movies accompany the paper, which we would like to be included as supporting online material. These have been sent to the editorial office by email, as they could not be uploaded into the online submission system.

Sincerely yours,

Matthias Hennig and Florentin Wörgötter

1
2
3
4
5
6
7
8
9
10
11
12
13
14
15
16
17
18
19
20
21
22
23
24
25
26
27
28
29
30
31
32
33
34
35
36
37
38
39
40
41
42
43
44
45
46
47
48
49
50
51
52
53
54
55
56
57
58
59
60
61
62
63
64
65

On the effect of fixational eye movements on the expression of retinal ganglion cell nonlinearities

Matthias H. Hennig¹ and Florentin Wörgötter^{2,3}

¹ANC, School of Informatics, University of Edinburgh, Edinburgh, EH1 2QL, UK

²Computational Neuroscience, BCCN, University of Goettingen, Bunsenstr. 10, 37073 Goettingen, Germany

³Computational Neuroscience, Department of Psychology, University of Stirling, Stirling, FK9 4LA, UK

Abbreviated Title: Ocular micromovements and retinal nonlinearities

Key words: Motion Perception, Eye Movements, Fixation, Model, Retina, Non-linearities, Magnocellular Pathway

Correspondence:

Matthias H. Hennig

ANC, Informatics

University of Edinburgh

Edinburgh, EH1 2QL

UK

Phone: +44 (0)131 650 3080, FAX: +44 (0)131 650 6899

Email: mhennig@inf.ed.ac.uk

March 26, 2007

1
2
3
4
5
6
7
8
9 **Abstract**

10 Psychophysical evidence suggests that during fixation involuntary eye
11 movements can lead to powerful illusions of apparent motion and other
12 instabilities. In this work, we used a detailed biophysical model of the
13 mammalian retina to investigate potential effects of fixational eye move-
14 ments on retinal ganglion cell activity during fixation of a star-shaped
15 stimulus. The model simulates the population activity of linear, sustained
16 (parvocellular) and nonlinear, transient (MC) ganglion cell type, and we
17 investigated the spatio-temporal activity patterns of these cell types. We
18 found two very distinct effects: a fading of complete wedges of the star
19 and an apparent splitting of stimulus lines. These effects only occur in
20 the MC-cell population and resemble the perceived instabilities during
21 fixation of a star-shaped or related stimuli. The analysis of simulated
22 single cell activity shows that fading effect is caused by an expression of
23 the aperture problem in retinal ganglion cells, and the splitting effect is a
24 result of spatio-temporal nonlinearities in MC-cells. We therefore propose
25 that certain illusory percepts may be traced back to specific properties of
26 retinal ganglion cell responses.
27

28 **1 Introduction**
29

30 Visual perception is initiated by the responses of large populations of neurons
31 in the retina. Usually, individual specific response properties of a given neuron
32 class cannot anymore be rediscovered at the perceptual level. Instead they
33 disappear in higher visual areas due to integration and other mechanisms which
34 facilitate the correct interpretation of a stimulus.
35

36 A famous example of this kind is the *aperture problem* (Wallach, 1935; Hil-
37 dreth and Koch, 1987). The area where a neuron in the visual system is excitable
38 by a stimulus is constrained by the finite dimensions of its receptive field, the
39 neuron’s window or aperture to the outer world. If an elongated stimulus (e.g.
40 a long bar) is passing over such a visual receptive field, the neuron will only
41 respond to the motion component which is orthogonal to the orientation of the
42 stimulus, while axial components do not contribute. This effect occurs essen-
43 tially for all cells at lower visual processing stages where receptive fields are
44 small. It considerably limits the ability of individual neurons to reliably encode
45 stimulus properties. On the other hand, the activity of a subset of neurons usu-
46 ally provide sufficient information to resolve these ambiguities at higher levels.
47 It has, for instance, been demonstrated that the aperture problem is resolved
48 by spatiotemporal integration the motion sensitive area MT (Pack and Born,
49 2001).
50

51 While this is only one example, large scale integration effects are thought
52 to be generally involved in the generation of stable visual percepts and the
53 individual cell properties over which integration takes place remain, therefore,
54 normally hidden. As a consequence the cellular properties of the dominant early
55 visual processing streams, the parvo- (MC) or magnocellular (PC) systems, are
56 not easily discovered at the perceptual level anymore. The segregation of these
57
58

1
2
3
4
5
6
7
8
9 two pathways begins in the retina and was first described for the cat retina.
10 Two types of ganglion cells were discovered, one showing linear (X-cells) and
11 the other nonlinear spatial summation (Y-cells) (Enroth-Cugell and Robson,
12 1966; Hochstein and Shapley, 1976; Victor, 1988).

13 In primates, the parvocellular stream is represented by linear, sustained
14 PC-cells and the magnocellular stream by MC-cells, which show fast, transient
15 responses and, albeit weaker than in the cat retina, nonlinear spatio-temporal
16 summation (Leventhal et al., 1981; Kaplan and Shapley, 1982; Derrington and
17 Lennie, 1984; Benardete et al., 1992). Furthermore, PC-cells have smaller re-
18 ceptive fields and a higher density than MC-cells, and only PC-cells have colour-
19 opponent receptive fields. It is therefor often hypothesised that PC-cells mediate
20 high-acuity vision for static stimuli while MC-cells are mainly involved in the
21 processing of moving stimuli (Schiller and Logothetis (1990); but see Lee et al.
22 (1993)).

23
24 These two cell classes provide the basis for the segregation into the ventral
25 and dorsal visual pathways, which have been associated to form- and motion-
26 analysis in the visual cortex (Merigan and Maunsell, 1993). Evidence how this
27 segregation affects perception is sparse and has so far been indirectly deduced,
28 mainly from lesioning or anatomical studies, and the results are still controver-
29 sial (Schiller and Logothetis, 1990; Gegenfurtner, 2003).

30 In spite of this, in this paper we will suggest that two visual illusions, which
31 are caused by fixational eye movements, may be directly related to specific
32 properties of the magnocellular retinal pathway. To show this, we simulated
33 responses of linear, sustained (PC) and nonlinear, transient (MC) ganglion cells
34 during stimulation with a star-shaped stimulus in the presence of fixational
35 eye movements. We found two effects in the populations response of MC-cells,
36 which strongly resemble visual illusions experienced for similar stimuli: a fading
37 of lines or whole wedges of the stimulus, and an apparent splitting of single
38 lines. Based on properties of simulated population activity, we will show that
39 both effects are induced by fixational eye movements and can be traced back
40 to specific properties of the retinal magnocellular system. These results suggest
41 that certain visual illusions may unmask specific properties of the magnocellular
42 pathway and could be manifested already at the level of retinal ganglion cell
43 responses.
44

45 46 **2 Materials and Methods**

47 48 **2.1 Structure of the model retina**

49
50 The model aims to simulate responses of populations of two types of retinal gan-
51 glion cells: a linear, sustained type with a small receptive field and a nonlinear,
52 transient type with a larger receptive field. The specific parameters for each cell
53 class were chosen, where possible, to reflect those of the primate foveal parvocel-
54 lular (PC) and magnocellular (MC) On-centre channels under cone-dominated
55 illumination conditions. It will be shown that important features of these neu-
56
57
58

rons are well captured by this model. Therefore, we refer to the two types as PC- and MC-cells throughout this study. The model was largely based on an earlier model used to explore differences in X- and Y-cell behaviour in the cat retina (Hennig et al., 2002). The limitations of the model will be addressed in the Discussion.

A schematic diagram of the connectivity of the model neurons is shown in Figure 1A. Model neurons are arranged on two-dimensional, stacked hexagonal grids. The photoreceptor layer consists of 200 X 200 neurons, with a nearest-neighbour separation of $0.55'$. Stimuli are first convolved with a point spread function to account for the ocular optics (Fig. 1B; Westheimer (1986)). Horizontal and bipolar cells receive synaptic input from photoreceptors. The horizontal cell layer was modelled as an electrically coupled syncytium and the activity is calculated at each site of synaptic contact to bipolar cells. A transient and sustained On-centre bipolar cell type was included, with the same density as the photoreceptors (Milam et al., 1993; Wässle and Boycott, 1991; Dacey, 1993). Both sustained and transient bipolar cells receive excitatory input from photoreceptors and are inhibited by horizontal cells. In addition, transient bipolar cells receive recurrent inhibition from amacrine cells which leads to an amplification of transient response characteristics (Fig. 1C). PC ganglion cells receive synaptic input from sustained and MC-cells from transient bipolar cells. Furthermore, both ganglion cell types receive inhibitory input from wide field amacrine cells, which contributes to their receptive field surround (Flores-Herr et al., 2001; Sinclair et al., 2004). Figure 1C illustrates representative responses of the sustained and transient pathway in the model.

In summary, this connectivity, which will be described in more detail below, produces the typical receptive fields of ganglion cells composed of a Gaussian-shaped excitatory centre and a wider surround. The temporal dynamics and gain of PC-cells closely follows that of the photoreceptors, whereas MC-cells are transient and show nonlinear spatio-temporal summation.

2.2 Neuron models and synaptic connectivity

Neurons were implemented according to the equation for a passive neural membrane given by:

$$C \frac{dV(t)}{dt} = \left(\sum_{i=0}^N g_i(t) \cdot (V(t) - E_i) \right) + \frac{V_{rest} - V(t)}{R}, \quad (1)$$

where C is the membrane capacitance, $g_i(t)$ the conductance evoked by input i , E_i its reversal potential, R the membrane resistance and V_{rest} the resting potential. To simplify the model, the following common set of parameters were used for all neurons: $C = 100pF$, $R = 100M\Omega$ and $V_{rest} = -60mV$. For excitatory (glutamatergic) inputs the reversal potential was $E_{rev,glu} = 0mV$, and for inhibitory input, it was set to $E_{rev,GABA} = -70mV$ for GABAergic and $E_{rev,gly} = -80mV$ for glycinergic synapses.

Synaptic conductances were modelled as linear functions of the presynaptic potential, expressed as $g_i(t) = f(V_{pre}) \cdot 0.3nS/V$ for all cell types except for transient bipolar cells, where $g_{i,T}(t) = f(V_{pre}) \cdot 0.4nS/V$ was used (see below). The glutamate release for bipolar and amacrine cells was truncated at $-3mV$ below resting potential (assuming a low maintained transmitter release):

$$f(t) = \frac{V_{pre}}{1 + \exp\left(-\frac{V_{pre}-3mV}{10mV}\right)} \quad (2)$$

Photoreceptors Cone photoreceptor responses under photopic conditions were simulated by means of a state-variable description. This is based on a model description of the photocurrent of macaque cones after brief stimulation (Schnapf et al., 1990), which was extended to calculate the corresponding photovoltage during light stimulation. The following set of equations describe the model:

$$\tau_{Casc} \frac{dS_i(t)}{dt} = S_{i-1}(t) - S_i(t), \quad (3)$$

$$\frac{d[cGMP](t)}{dt} = \underbrace{-\beta \cdot ([Ca^{2+}](t) - 1)}_{\text{resynthesis}} - \underbrace{S_3(t) \cdot [cGMP](t)}_{\text{stimulus induced}}, \quad (4)$$

$$\frac{d[Ca^{2+}](t)}{dt} = \underbrace{\gamma(1 + c \cdot ([cGMP](t) - 1))}_{\text{influx}} - \underbrace{\alpha \cdot [Ca^{2+}](t)}_{\text{efflux}}. \quad (5)$$

$$\frac{d[H](t)}{dt} = \left(\frac{1}{e^{(V_P(t)-A_H)S_H} + 1} \right) \cdot (1 - [H](t)) - \delta_H[H](t), \quad (6)$$

$$C_P \frac{dV_P(t)}{dt} = q_P \frac{d[Ca](t)}{dt} + q_I \frac{d[H](t)}{dt}, \quad (7)$$

Parameters and their description are given in Table 1. This model reproduces the time course of the photovoltage during light stimulation as described by (Schnapf et al., 1990), produces a Michaelis Menten intensity-response relation and follows Weber's law for background desensitisation (Hennig et al., 2002). The photovoltage response of the model is biphasic with a sharp onset transient hyperpolarisation, which is followed by a weaker sustained response. The response terminates due to action of an inward hyperpolarisation-activated current with a transient depolarisation (Eqn. 6), which is slower and slightly weaker than the initial onset transient (Fig. 1C). For a complete description and discussion of this photoreceptor model, see Hennig et al. (2002) (note there is a mistake in Eqn. 4 in that paper).

1
2
3
4
5
6
7
8
9 **Horizontal cells** Horizontal cells were simulated as a syncytium of electrically
10 coupled neurons. The spatial decay of the activity was assumed to be Gaussian
11 shaped. The standard deviation was set to four cone diameters, about the size
12 of the midget cell receptive field surround in the fovea (Wässle et al., 1989).
13 Hence these horizontal cells best reflect the achromatic H1 population, which
14 is held responsible for shaping midget bipolar cell receptive fields (Dacey et al.,
15 2000; McMahan et al., 2004).
16

17 **Bipolar cells** The model includes two types of bipolar cells: sustained and
18 transient On-centre bipolar cells (see representative responses in Fig. 1C). All
19 bipolar cell types receive sign-inverted excitatory input from cones (Masu et al.,
20 1995) and are antagonised by horizontal cells to account for their receptive field
21 surround (Dacey et al., 2000; McMahan et al., 2004). This was simulated by
22 inverting the horizontal cell activity and assuming a synapse with a reversal
23 potential at $E_{rev,inh} = -70mV$ (Feigenspan et al., 1993). When voltage-gated
24 currents in cones/bipolar cells are neglected, this implementation is mathemati-
25 cally equivalent to both a non-GABAergic mechanism which relies on the voltage
26 modulation in the synaptic cleft (Kamermans and Spekreijse, 1999) or on an
27 increase of the Cl^- reversal potential above the resting potential in the cone
28 axon or bipolar dendrites (Vardi et al., 2000).
29

30 In addition, transient bipolar cells receive GABAergic inhibition from narrow-
31 field amacrine cells at their axon terminals (see below). This input is part of a
32 circuit which leads to more transient responses. Also, their input conductance
33 was increased by a factor of 1.3 to compensate for the reduced transient com-
34 ponent due to inhibition in transient bipolar cells (which also leads to a slight
35 increase in gain).
36

37 **Amacrine cells** The axon terminal of transient bipolar cells receives inhi-
38 bition from a narrow-field amacrine cell, which is part of a nested amacrine
39 circuit (shaded region in Fig. 1A). These narrow-field amacrine cells receive ex-
40 citatory input from a single bipolar cell and are inhibited by wide-field amacrine
41 cells. Inhibitory wide-field amacrine cells receive excitatory input from transient
42 bipolar cell terminals and are in turn inhibited by narrow field amacrine cells.
43 A narrow-field amacrine cell receptive field centre is therefore equivalent to the
44 bipolar cell receptive field, and that of wide-field cells Gaussian shaped with a
45 radius of 2.5 cone diameters ($\sigma_C=1.4'$).
46

47 This circuit reduces the sustained component of transient bipolar cells by
48 means of delayed inhibition. The onset transient is further amplified by wide-
49 field amacrine cells, which then act in a disinhibitory way. This effect is partic-
50 ularly pronounced for larger stimuli that excite wide-field amacrine cells fully.
51 Experimental results suggest that an equivalent amacrine cell circuit contributes
52 to the transient responses of ganglion cells (Nirenberg and Meister, 1997; Roska
53 et al., 1998). While this specific model is based on data obtained in the sala-
54 mander retina (Roska et al., 1998), data from the cat retina suggests that an
55 equivalent circuit may exist in mammals (O'Brien et al., 2003).
56
57
58

1
2
3
4
5
6
7
8
9 A further type of amacrine cell was included as an inhibitory interneuron
10 with a wide receptive field that contributes to the ganglion cell receptive field
11 surround. These cells receive excitatory input from bipolar cells and inhibit
12 ganglion cells (Flores-Herr et al., 2001; Sinclair et al., 2004). The Gaussian
13 radius of their receptive fields was set to 3.8 times the centre size of the respective
14 postsynaptic ganglion cell.
15

16 **Ganglion cells** PC-cells were separated by $0.55'$ and MC-cells by $1.65'$ on
17 the hexagonal retinal grid (Dacey and Petersen, 1992; Goodchild et al., 1996).
18 For MC-cells this value reflects a coverage factor of one (Wässle and Boycott,
19 1991; Dacey, 1993) for a dendritic tree diameter of about $6'$ (Goodchild et al.,
20 1996). Another study has reported higher values (Dacey and Petersen, 1992),
21 but wider receptive fields were not considered. PC-cells receive excitatory input
22 from a single sustained bipolar cell and MC-cells from seven transient bipolar
23 cells. The inhibitory surround is mediated by wide field amacrine cells with a
24 receptive field of > 3.8 times the centre input (Flores-Herr et al., 2001; Croner
25 and Kaplan, 1995; Lee et al., 1998).
26

27 It should be noted that the receptive field dimensions specified above re-
28 flect the anatomical connectivity, and that the effective physiological receptive
29 field is larger due to optical blurring and the presynaptic circuitry. Consistent
30 with experimental data (Croner and Kaplan, 1995; Lee, 1996), the physiological
31 centre radius of simulated foveal PC- and MC-cells, when tested with drifting
32 grating stimuli, is very similar (not illustrated).
33

34 Due to their connectivity, simulated PC-cells effectively inherit their re-
35 sponse characteristics from photoreceptors after spatio-temporal filtering (Fig. 1C,
36 compare photoreceptor, bipolar and PC-cell responses). In contrast, the re-
37 sponse of MC-cells is strongly influenced by the action of the nested amacrine
38 circuit, which leads to the pronounced transient behaviour (Fig. 1C, compare
39 photoreceptor, transient bipolar and MC-cell responses).
40

41 2.3 Optical blurring

42 Optical blurring was simulated by convolving the stimulus with a point spread
43 function (PSF) given by (Westheimer, 1986) for the human fovea:
44

$$45 \quad PSF(\rho) = 0.933 \cdot e^{-2.59 \cdot \rho^{1.36}} + 0.047 \cdot e^{-2.34 \cdot \rho^{1.74}}, \quad (8)$$

46 where ρ denotes the visual angle in minutes of arc. The PSF is illustrated in
47 Figure 1B.
48
49

50 2.4 Ocular micromovements

51 Simulated fixational eye movements include slow drift movements and the ocular
52 microtremor, which were generated by a multiplication of Fourier-transformed
53 white noise with a characteristic power spectrum. The power spectrum of the
54 microtremor was modelled as Gaussian normal distribution with a peak at 80
55
56
57
58

1
2
3
4
5
6
7
8
9 Hz and standard deviation of 25 Hz (Bolger et al., 1999; Spauschus et al., 1999).
10 For the ocular drift, following Eizenman et al. (1985) the following expression
11 for the power spectrum was used:

$$12 \quad P(f) = \frac{A}{(1 + T_1 f)^2 \cdot (1 + T_2 f)^2} \quad (9)$$

13
14
15 where $f[Hz]$ is the frequency. The variables were $T_2 = 0.1s$, $A = 3000''$ and
16 $T_1 = 1.3s$, and the tremor was superimposed onto the drift spectrum. The
17 resulting simulated eye movements consist of the tremor with a mean amplitude
18 of $15'' - 20''$ (Riggs and Ratliff, 1951; Ditchburn and Ginsborg, 1953; Steinman
19 et al., 1973) and drift movements with a mean amplitude of $6.5'$ and a mean
20 velocity of 0.5 deg/s (Murakami, 2004).
21
22

23 **2.5 Stimulus**

24
25 A static star shaped stimulus at 100% contrast with a diameter of $110'$ and 24
26 bars, each $2.86''$ wide.
27

28 **2.6 Simulations**

29
30 The simulation software was implemented in C++ and simulations were per-
31 formed on a cluster of Intel x86/Linux computers. Numerical integration was
32 performed in double precision using the second order Runge Kutta method with
33 a time step of $100\mu s$, which allowed for an accurate simulation of cone responses
34 in the presence of the fast ocular microtremor.
35
36

37 **3 Results**

38 **3.1 Simulated ganglion cell activity**

39
40 The activity of ganglion cells was simulated during fixation of a star shaped
41 stimulus (Fig. 3A). Small eye-movements were included to simulate a physio-
42 logical fixation condition (Fig. 3B). In the following, a representative episode
43 of the population response lasting 250ms will be analysed which illustrate the
44 main effects. Longer movies of these activity patterns are available as support-
45 ing online material.
46

47 Snapshots of the ganglion cell activity, taken at two different times t_1 and
48 t_2 (as indicated in Fig. 3B), are shown in Figure 3C-F. The top panels (Fig. 3C,D)
49 show PC-cell, those on the bottom (E,F) MC-cell responses. At time t_1 , the eye
50 movement direction is approximately vertical, top to bottom, which changes to
51 bottom-right at t_2 (arrows in Fig. 3B).
52

53 Both at t_1 and t_2 , and for both cell types, the bars of the stimulus cause
54 depolarising responses (colour-coded red in Fig. 3C-F). The stimulus motion
55 also leads to a trailing hyperpolarisation (colour-coded blue), which is caused
56
57
58

1
2
3
4
5
6
7
8
9 by stimulation of the receptive field surround. This is the expected behaviour
10 of ganglion cells, which respond to local changes in contrast.

11 A comparison of PC- and MC-cell response patterns however clearly shows
12 that the activity of MC-cells is strongly reduced in two sectors, which are located
13 along one axis of the stimulus. The orientation of this axis changes as the
14 direction of the eye movements change from vertical to oblique. This change
15 is gradual over time and very pronounced in MC-cells, but also, albeit much
16 weaker, visible in PC-cells (compare E, F and C,D). In PC-cells, the membrane
17 potential in the sectors with a reduced response is reduced to about 50% of the
18 peak activity. In MC-cells, the responses in these sectors are reduced almost to
19 resting potential.

20 In addition, a second effect is visible in the simulated MC-cell population
21 response in Figure 3E and F. The snapshot of the MC-cell population activity
22 taken at t_2 (Fig. 3F) shows that some lines display a spatially separated activity
23 towards the periphery, which does not correspond to any part of the stimulus.
24 Instead of the regular pattern of the stimulus, one finds pairs of depolarising
25 lines next to each other. This effect does not occur in the PC-cell population.

26 The comparison of the membrane potential traces details this observation
27 (Fig. 3H). Photoreceptors and PC-cells show two moving, spatially separated
28 activity peaks, which correspond to two lines of the stimulus. The same peaks
29 are found in the MC-cells. Between both real peaks, however, MC-cell responses
30 show a smaller additional activity peak (marked by diamonds).

31 We note here that both effects can indeed be experienced during careful
32 fixation of a star-shaped stimulus. The strength of the effect however varies
33 from person to person and depends on specific stimulus parameters (see Discus-
34 sion). The results presented here could therefore guide further psychophysical
35 or electrophysiological experiments.
36
37

38 39 **3.1.1 Line-fading**

40 How are eye-movements and direction of the “fading” of star-segments related?
41 In the transition from the first snapshot in Figure 3 at t_1 to the second at t_2 ,
42 eye movement direction has changed from approximately vertical to bottom-
43 right (arrows in B). Thus, in both situations, fading occurs in sectors parallel
44 to the eye-movement direction.

45 The diagrams in panel G of show the activity of modelled photoreceptors,
46 PC-cells and MC-cells for cells taken from the cross-section marked by the red
47 bar in panel A. The receptive fields of the cells in the middle row (G, aster-
48 isks) are those stimulated by the line of the stimulus marked by an asterisk in
49 A. Motion of this line is approximately axial, thus the spatial stimulation of
50 the corresponding receptive fields does not change much during this interval.
51 Both PC- and MC-cells at this location first respond with a depolarisation as
52 the stimulus enters their receptive field. But after about 40ms, their activity
53 is reduced to a lower steady-state level (asterisks in G). This is particularly
54 pronounced for MC-cells and explains the observed strong activity drop in the
55 MC-cell population.
56
57
58

1
2
3
4
5
6
7
8
9 Strictly speaking, this effect might be interpreted as an expression of the
10 aperture problem at the level of retinal ganglion cells. The model responses
11 suggest that MC-cells are susceptible to the aperture problem due to their tran-
12 sient nature — but while their response does not encode the direction of stimulus
13 motion, axial motion will lead to a weak response. As higher motion-sensitive ar-
14 eas mainly receive input from the dorsal stream (Schiller and Logothetis, 1990),
15 a stimulus under these conditions may therefore remain “invisible” to the visual
16 cortex. Fixational eye movements will normally prevent this effect by providing
17 additional motion to stimulate adjacent receptive fields, but for stimuli with
18 large homogeneous structures like the star used here, may be the source of a
19 false percept.
20

21 **3.1.2 Line-splitting**

22
23 The apparent splitting of lines of the stimulus in the mode arises from the non-
24 linear properties of MC-cells which also can lead to frequency-doubled responses
25 during stimulation with contrast-reversed gratings (Kaplan and Shapley, 1982;
26 Benardete et al., 1992). Frequency-doubling refers to the effect that certain MC-
27 cells respond with a transient depolarisation to a stimulus that reverses its con-
28 trast, but is otherwise spatially fully balanced over the receptive field (see Demb
29 et al. (1999) for a good summary).
30

31 During fixation of the star stimulus, fixational eye-movements may move
32 two stimulus lines across opposite parts of a single MC-cell receptive field. In
33 this case, the geometry of the stimulus can lead to a situation where as one
34 line enters the receptive field at one side, the second line leaves it on the other
35 side, effectively producing a zero net excitation of the receptive field. A linearly
36 summing ganglion cell located between both bars will then not respond.

37 If however, as for MC-cells, the receptive field includes nonlinear spatial
38 summation, a response may be expected in this situation. Figure 4 provides a
39 detailed illustration of this effect: The photoreceptor responses in A represent a
40 case where one bar leaves and the other enters a MC-cell receptive field. Panel B
41 shows numerically differentiated photoreceptor responses, highlighting the on-
42 and offset-responses. This is a simplification that in this form is not computed
43 by the full model, but illustrates best what happens. On- and off-transients in
44 photoreceptors are of different temporal kinetics and magnitude, and therefore
45 summation across the wide MC-receptive field (panel D) leads to a small remain-
46 ing “ghost” activity at a location without a physical stimulus. This response is
47 superimposed, after scaling, inverting and applying a low-pass filter, onto the
48 full MC-cell model response in panel C. The good match indicates that in a
49 first approximation line-splitting can be understood from the amplification and
50 integration of imbalanced photoreceptor transients. As suggested earlier (Hen-
51 nig et al., 2002), in this model the amplification of photoreceptor-asymmetries
52 results from an inhibitory amacrine cell circuit. Note that this effect can not
53 occur for moving grating stimuli, as they will not produce the required balanced
54 On- and Off-stimulation of a single receptive field.
55
56
57
58

1
2
3
4
5
6
7
8
9 **3.1.3 Differential effects of different sources of nonlinearities for line-**
10 **splitting**

11 To investigate the role of the different factors contributing to the nonlinear be-
12 haviour of simulated MC-cells to the line-splitting effect, Figure 5 shows snap-
13 shots of the ganglion cell population response for the original model and after
14 certain modifications. Parts A and B show responses of unmodified PC- and
15 MC-cells, respectively. The stimulus was presented at a higher luminance than
16 in Figure 3, and in this particular example, eye movements led mainly to a
17 “rotational” movement of the stimulus with little on-axis movement. Accord-
18 ingly, the line-fading effect weak, but line-splitting is visible in the MC-cell
19 response (circle in B).
20

21 Part C shows the MC-cell response after replacing the original photoreceptor
22 model with a “linearised” variant, which consists of a cascaded low-pass filter
23 and a Michaelis-Menten saturation characteristic. In this case line-splitting is
24 reduced, indicating that photoreceptor response asymmetries play a role in gen-
25 erating the nonlinear response. It is however not fully abolished, indicating
26 additional sources of nonlinear spatio-temporal summation. This change is sim-
27 ilar to the effect of a linear photoreceptor on the frequency-doubling response for
28 contrast-reversed gratings in this type of model, as demonstrated earlier (Hennig
29 et al., 2002).
30

31 Part D shows an example where the nested amacrine circuit, which leads
32 to transient responses in MC-cells, was inactivated. This modification leads to
33 a complete abolishment of the line-splitting effect. In addition, the response
34 amplitudes of the ganglion cells are weaker than for the full model, which re-
35 sults from the lack of amplification of onset-transients. Hence, in this model,
36 the combination of inhibition and disinhibition caused by the nested amacrine
37 circuit (see Hennig et al. (2002) for details) is the main factor that leads to the
38 line-splitting effect.

39 This result is contrast to earlier findings that amacrine cells are not the
40 main source of receptive field nonlinearities causing the frequency-doubling ef-
41 fect (Demb et al., 1999, 2001a). An earlier modelling study suggested that the
42 degree of responses nonlinearity depends, on the size of the receptive field of a
43 nonlinear ganglion cell, if expressed in terms of the number of converging pho-
44 toreceptors or bipolar cells (Hennig et al., 2002). This suggestion is consistent
45 with the experimental result that frequency-doubling in nonlinear ganglion cells
46 is the result of the summation of asymmetric responses of bipolar cells (Demb
47 et al., 2001a).
48

49 The separation of the spokes of the star stimulus used here increases with
50 increasing eccentricity, and the splitting effect is visible for a separation of
51 $> 10' - 15'$. This is by far more than the total receptive field diameter of a
52 simulated MC-cell (about $10'$ in this case), therefore MC-cells will not directly
53 receive asymmetric responses from bipolar cells. Instead, the apparent splitting
54 of the lines of the stimulus is caused by the wide-field amacrine cells, which con-
55 tribute to the response of a given ganglion cell beyond its anatomical receptive
56 field. A similar influence on simulated responses to contrast-reversed gratings
57
58
59
60
61
62
63
64
65

1
2
3
4
5
6
7
8
9 in nonlinear ganglion cells is also visible at low spatial frequencies (see Fig. 7 in
10 Hennig et al. (2002)).

11 This effect is further illustrated in Figure 5E, where the responses of MC-cells
12 receiving excitatory input from only a single photoreceptor are shown, but where
13 the size of the amacrine cell receptive fields was unchanged. The splitting effect
14 is in this case even more pronounced than for a larger receptive field, because
15 the smaller receptive fields also reduce spatial blurring of the stimulus.

16 Summarising, the simulation results show that the line-splitting effect is
17 caused by nonlinearities in the inner retina, which form a part of the extra-
18 classical receptive field of MC-cells. This result leads to the prediction that
19 in an electrophysiological experiment, the line-splitting effect should be largely
20 abolished in the presence of antagonists that block inhibition in the inner retina.
21 In addition, it may be expected that TTX-sensitive long-range inhibition in the
22 inner retina by spiking amacrine cells, which has been shown to contribute to
23 the frequency-doubling response in nonlinear ganglion cells (Demb et al. (1999);
24 not included in this model), may contribute to line-splitting in a similar way.
25
26

27 4 Discussion

28
29 In this paper, a computational model of the parvo- and magnocellular channels
30 in the primate retina was used to assess possible effects of ganglion cell non-
31 linearities on the spatial representation of a visual stimulus in the presence of
32 fixational eye movements (ocular microtremor and slow drift). The population
33 response of retinal ganglion cells to a star-shaped stimulus was investigated, and
34 two distinct effects were found in the stimulus representation in the magnocel-
35 lular stream: fading of complete wedges and an apparent splitting of stimulus
36 lines. It was shown that both effects, which do not appear in the parvocellular
37 stream, are initiated by fixational eye movements and result from the nonlinear
38 nature of magnocellular ganglion cells. Sectorial fading during fixation of a star
39 is caused by transient character of MC-cells, and apparent splitting of lines of
40 the stimulus by nonlinear spatio-temporal summation in the MC-cell receptive
41 field. Qualitatively similar effects are reported by observers viewing this type of
42 stimulus (see below), and we propose here that their origin may be traced back
43 to specific properties of retinal magnocellular ganglion cells.
44

45 The results in this paper allow for specific predictions for possible psy-
46 chophysical and electrophysiological experiments. Reported fading of lines in a
47 star-shaped stimulus as well as an apparent splitting of lines should correlate
48 with the direction of recorded eye movements, and should be visible in multi-
49 electrode array recordings in retinal in-vitro assays. As will be discussed next,
50 these predictions are based on very general properties of retinal ganglion cell
51 responses, and the necessary requirements on the mechanisms producing these
52 effects are well supported by the existing experimental data.
53
54
55
56
57
58

4.1 Validity of the modelling results

As described, the fading of sectors of the stimulus essentially relies on the transient responses, a well-documented feature of MC-cells (Lee et al., 1990). In this model, it was assumed that a combination of recurrent amacrine cell inhibition (and disinhibition; see Methods) and higher synaptic gain of bipolar cells produces the transient behaviour, a mechanism inspired by findings in the salamander retina (Nirenberg and Meister, 1997; Roska et al., 1998). To our knowledge, no experimental studies exist to date that address this issue in the primate retina, but experiments in the cat retina suggest that either alpha-ganglion cells or bipolar cell terminals receive glycinergic inhibition from amacrine cells which in turn receive GABAergic inhibition (O'Brien et al., 2003). These results are consistent with our model of a nested amacrine circuit, which specifically affects MC-cell responses. On the other hand, a study in the salamander retina also demonstrated that cell-intrinsic factors can contribute to transient responses in bipolar cells (Awatramani and Slaughter, 2000), rendering it more likely that transient behaviour of ganglion cells has multiple origins in the presynaptic circuitry. Despite all this, the fading-effect proposed here for MC-cells is expected to occur in all scenarios where transient behaviour occurs for stimuli with dimensions similar to the receptive field diameter, and hence the precise method of simulating transient responses should have little impact on the predicted behaviour.

The apparent splitting of lines of the stimulus observed in the model relies on nonlinear spatio-temporal summation, which causes a ganglion cell to respond to stimuli which cause no net excitation of their receptive field. This effect is therefore related to the frequency-doubling response for contrast-reversed gratings, as originally described for cat Y-cells (Enroth-Cugell and Robson, 1966) and later in the primate LGN (Kaplan and Shapley, 1982). In response to sinusoidally modulated contrast reversal, the simulated MC-cells in this paper have a mean nonlinearity index (the amplitude of the second divided by first harmonic response, measured at the spatial phase with maximal modulation) of 0.51 ± 0.15 in a range of spatial frequencies between 0.5-16 cpd. Consistent with experimental results, the nonlinearity index increases as the spatial frequency is increased further (data not shown; White et al. (2002)). Hence the behaviour of these cells is consistent with the majority of MC-cells in the primate retina, which exhibit a nonlinearity index less than one (White et al., 2002).

The origin of spatio-temporal nonlinearities in ganglion cells is not fully understood. Experimental data suggests that (1) amacrine cell involvement is less important (Demb et al., 1999), and (2) frequency-doubled activity might result from summation of spatially asymmetric bipolar cell activity (Demb et al., 2001a). The latter mechanism is the basis for spatio-temporal nonlinear behaviour of MC-cells in the model used in this study. As discussed in detail in an earlier paper, the spatial asymmetry of bipolar cell responses may result from a combination of photoreceptor response kinetics and the influence of amacrine cells (Hennig et al., 2002). It should however be noted that the line-splitting effect strongly depends on the nested amacrine circuit (see Fig. 5), as it is elicited

1
2
3
4
5
6
7
8
9 by stimuli located beyond the classical MC-cell receptive field.

10 As for the transient response, we note that the details of the mechanism
11 generating spatially asymmetric bipolar cell input are not crucial to produce the
12 line-splitting effect. Instead, this effect will always occur, as long as a ganglion
13 cell received a non-zero net input under conditions with zero net stimulation.
14 For instance, the extra-classical receptive field of Y-cells (Fisher et al., 1975;
15 Demb et al., 1999), which relies on long-range transmission not included in this
16 model, might further contribute to this effect.

17 Finally, we note that we have restricted our analysis to drift movements
18 and the ocular microtremor. Microsaccades are another form of fixational eye
19 movement, which occur infrequent during normal vision (Steinman et al., 1967).
20 Recent work indicates that microsaccades can induce correlations in retinal motion
21 on short time scales (Engbert and Kliegl, 2004) and their occurrence is
22 not random, but depends on the history of drift movements (Engbert and Mer-
23 genthaler, 2006). In addition, microsaccades strongly influence the responses
24 of visual neurons (reviewed in Martinez-Conde et al. (2004)). Therefore, it
25 seems likely that microsaccades additionally influence the effects described in
26 the study. On the other hand, psychophysical studies of related visual illu-
27 sions (see below) indicate that mainly slow drift movements, not microsaccades,
28 might cause the relevant effects (Zanker, 2004; Zanker and Walker, 2004; Mu-
29 rakami et al., 2006).
30
31

32 4.2 Psychophysical correlates

33
34 During careful fixation of a star-shaped stimulus (similar to that shown in
35 Fig. 3A), two distinct effects can be observed, which are compatible with our
36 modelling results. Typically, a fading or disappearing of lines or sectors of the
37 stimulus occurs, which gradually changes its orientation and leads to apparent
38 motion percepts. Additionally, often an apparent splitting of individual lines is
39 visible. Both effects, in particular the latter, are short-lived and transient, and
40 immediately disappear after loss of precise fixation.

41 In a qualitative assessment, we presented the star stimulus to 35 naive sub-
42 jects asking them to provide a verbal description of their percept during fixation.
43 All observers reported that during fixation wedge-shaped sectors of this stimulus
44 begin to fade; most often in two wedges opposite to each other. The location of
45 the fading wedges rotates randomly, affecting all orientations. However, most
46 observers reported that the fading is particularly strong on an oblique axis.
47 The latter may be attributed to additional contribution from the “oblique ef-
48 fect” (Appelle, 1972), according to which horizontally and vertically oriented
49 stimuli are better seen than oblique structures.
50

51 In addition, 66% of the subjects (n=23/35) reported that lines appear to
52 split or that they become denser, as if lines have been “added in between close
53 to the centre”. Hence this illusion is less clear than the fading effect, which
54 was confirmed by all observers. Observers also consistently reported that the
55 percept is more short-lived than the line-fading.
56
57
58
59
60
61
62
63
64
65

1
2
3
4
5
6
7
8
9 These results suggest that the predicted effects might indeed lead to corre-
10 sponding visual illusions. This is however only a preliminary hypothesis, as this
11 experiment could neither establish the origin of the illusions nor were the ob-
12 server’s eye movements tracked to establish the proposed link between eye move-
13 ment direction and direction of fading or line-splitting. This study therefore
14 provides a basis for further experimental investigation of these effects. We note
15 that very similar effects have been reported earlier for other stimuli with a circu-
16 lar symmetry, such as for concentric circles by Purkinje and Helmholtz (Wade,
17 2003) and for the well-known MacKay Illusion (Pirenne et al., 1958).
18
19

20 **4.3 Relations to existing psychophysical observations**

21 Several impressive visual illusions exist which are elicited by retinal image mo-
22 tion due to eye-movements during fixation, some of which were first described by
23 Purkinje and Helmholtz (for a review, see Wade, 2003). More recently, a number
24 of related illusions were systematically studied and a clear link to fixational eye
25 movements has been established (Murakami et al., 2006). These aesthetically
26 appealing pictures, which have also influenced the arts (“Op-Art”), have also
27 been used to deduce possible neuronal mechanisms which underlie their percep-
28 tion. During fixation, observers report unstable flickering or apparent motion
29 percepts, which can affect the image as a whole or parts of it.
30

31 The aperture problem has been discussed in conjunction with these illusions
32 previously and models have been made to explain the Ouchi illusion (Mather,
33 2000; Fermüller et al., 2000) and others by means of simulated cortical motion
34 detectors (Zanker, 2004; Zanker and Walker, 2004). Our study augments these
35 findings by providing arguments for a retinal origin of these illusions. It is
36 conceivable that the apparent motion elicited by these illusions requires at some
37 point the activation of cortical motion detectors. Our results however indicate
38 that this percept may not be the consequence of specific properties of cortical
39 motion detectors.
40

41 **4.4 Implications for visual processing**

42 It is commonly agreed that the finely grained activity from lower visual areas
43 is integrated at higher levels of the processing hierarchy, and specific cellular
44 properties of early visual neurons are lost in this process. In this study we
45 propose that this principle may be violated and that stimulus conditions exist,
46 where retinal activity patterns appear to directly match a illusory visual percept.
47

48 To our knowledge, the line splitting effect described here might be the first
49 perceptual correlate of the frequency-doubling nonlinearity of MC-cell receptive
50 fields. [It should be noted that a clinically applied glaucoma test where the rapid
51 contrast reversal of a grating leads to the precept of doubled spatial frequency is
52 not a direct consequence of MC-cell frequency-doubling (White et al., 2002).] In
53 principle, our explanation for the splitting effect suggests that MC-cells have the
54 ability to encode spatiotemporal variations on a smaller spatial scale than their
55 classical receptive field allows. It has, for instance, been reported that Y-like
56
57
58

1
2
3
4
5
6
7
8
9 cells could provide cues to detect second-order motion (Demb et al., 2001b). It
10 may therefore be interesting to further investigate the influence of the MC-cell
11 nonlinearities on the analysis of stimulus conditions relevant in natural scenes.
12

13 **5 Acknowledgments**

14
15 We wish to thank Peter Hancock for advise on psychophysical studies and Hans
16 Ekkehard Plesser for the Matlab code to plot the population activity. This
17 work was supported by the European Commission grant “ECOVISION” and
18 the Scottish higher education grant to the “Institute for Neural Computational
19 Intelligence”.
20
21
22
23
24
25
26
27
28
29
30
31
32
33
34
35
36
37
38
39
40
41
42
43
44
45
46
47
48
49
50
51
52
53
54
55
56
57
58
59
60
61
62
63
64
65

References

- Appelle, S. (1972). Perception and discrimination as a function of stimulus orientation: the "oblique effect" in man and animals. *Psychol Bull*, 78(4):266–278.
- Awatramani, G. B. and Slaughter, M. M. (2000). Origin of transient and sustained responses in ganglion cells of the retina. *J Neurosci*, 20(18):7087–7095.
- Bader, C. R. and Bertrand, D. (1984). Effect of changes in intra- and extracellular sodium on the inward (anomalous) rectification in salamander photoreceptors. *J Physiol*, 347:611–31.
- Benardete, E. A., Kaplan, E., and Knight, B. W. (1992). Contrast gain control in the primate retina: P cells are not X-like, some M cells are. *Vis Neurosci*, 8:483–486.
- Bolger, C., Bojanic, S., Sheahan, N. F., Coakley, D., and Malone, J. F. (1999). Dominant frequency content of ocular microtremor from normal subjects. *Vision Res*, 39:1911–1915.
- Croner, L. and Kaplan, E. (1995). Receptive fields of P and M ganglion cells across the primate retina. *Vision Res*, 35(1):7–24.
- Dacey, D., Packer, O. S., Diller, L., Brainard, D., Peterson, B., and Lee, B. B. (2000). Center surround receptive field structure of cone bipolar cells in primate retina. *Vision Res*, 40:1801–1811.
- Dacey, D. and Petersen, M. (1992). Dendritic field size and morphology of midget and parasol ganglion cells in the human retina. *Proc Natl Acad Sci U S A*, 89:9666–9670.
- Dacey, D. M. (1993). The mosaic of midget ganglion cells in the human retina. *J Neurosci*, 13:5334–5355.
- Demb, J. B., Haarsma, L., Freed, M. A., and Sterling, P. (1999). Functional circuitry of the retinal ganglion cell's nonlinear receptive field. *J Neurosci*, 19(22):9756–9767.
- Demb, J. B., Zaghloul, K., Haarsma, L., and Sterling, P. (2001a). Bipolar cells contribute to nonlinear spatial summation in the brisk-transient (Y) ganglion cell in mammalian retina. *J Neurosci*, 21(19):7447–7454.
- Demb, J. B., Zaghloul, K., and Sterling, P. (2001b). Cellular basis for the response to second-order motion cues in Y retinal ganglion cells. *Neuron*, 32(4):711–721.
- Demontis, G. C., Longoni, B., Barcaro, U., and Cervetto, L. (1999). Properties and functional roles of hyperpolarization-gated currents in guinea-pig retinal rods. *J Physiol*, 515:813–828.

- 1
2
3
4
5
6
7
8
9 Derrington, A. M. and Lennie, P. (1984). Spatial and temporal contrast sen-
10 sitivities of neurones in lateral geniculate nucleus of macaque. *J Physiol*,
11 357:219–240.
- 12
13 Ditchburn, R. W. and Ginsborg, B. L. (1953). Involuntary eye movements
14 during fixation. *J Physiol*, 119(1):1–17.
- 15
16 Eizenman, M., Hallett, P. E., and Frecker, R. C. (1985). Power spectra for
17 ocular drift and tremor. *Vision Res*, 25:1635–1640.
- 18
19 Engbert, R. and Kliegl, R. (2004). Microsaccades keep the eyes’ balance during
20 fixation. *Psychol Sci*, 15(6):431–436.
- 21
22 Engbert, R. and Mergenthaler, K. (2006). Microsaccades are triggered by low
23 retinal image slip. *Proc Natl Acad Sci U S A*, 103(18):7192–7197.
- 24
25 Enroth-Cugell, C. and Robson, J. G. (1966). The contrast sensitivity of retinal
26 ganglion cells of the cat. *J Physiol*, 187:517–552.
- 27
28 Feigenspan, A., Wässle, H., and Bormann, J. (1993). Pharmacology of GABA
29 receptor Cl channels in rat retinal bipolar cells. *Nature*, 361:159–161.
- 30
31 Fermüller, C., Pless, R., and Aloimonos, Y. (2000). The Ouchi illusion as an
32 artifact of biased flow estimation. *Vision Res*, 40(1):77–96.
- 33
34 Fisher, J., Krger, J., and Droll, W. (1975). Quantitative aspects of the shift
35 effect in cat retinal ganglion cells. *Brain Res*, 83:391–403.
- 36
37 Flores-Herr, N., Protti, D. A., and Wässle, H. (2001). Synaptic currents gen-
38 erating the inhibitory surround of ganglion cells in the mammalian retina. *J*
39 *Neurosci*, 21(13):4852–4863.
- 40
41 Gegenfurtner, K. R. (2003). Cortical mechanisms of colour vision. *Nat Rev*
42 *Neurosci*, 4(7):563–572.
- 43
44 Goodchild, A. K., Ghosh, K. K., and Martin, P. R. (1996). Comparison of
45 photoreceptor spatial density and ganglion cell morphology in the retina of
46 human, macaque monkey, cat, and the marmoset callithrix jacchus. *J Comp*
47 *Neurol*, 366:55–75.
- 48
49 Hennig, M. H., Funke, K., and Wörgötter, F. (2002). The influence of different
50 retinal subcircuits on the nonlinearity of ganglion cell behavior. *J Neurosci*,
51 22(19):8726–8738.
- 52
53 Hildreth, E. C. and Koch, C. (1987). The analysis of visual motion: from
54 computational theory to neuronal mechanisms. *Annu Rev Neurosci*, 10:477–
55 533.
- 56
57 Hochstein, S. and Shapley, R. M. (1976). Linear and nonlinear spatial subunits
58 in Y cat retinal ganglion cells. *J Physiol*, 262:265–284.

- 1
2
3
4
5
6
7
8
9 Kamermans, M. and Spekreijse, H. (1999). The feedback pathway from horizontal cells to cones. A mini review with a look ahead. *Vision Res*, 39(15):2449–2468.
- 12 Kaplan, E. and Shapley, R. M. (1982). X and Y cells in the lateral geniculate nucleus of macaque monkeys. *J Physiol*, 330:125–143.
- 15 Lee, B. (1996). Receptive field structure in the primate retina. *Vision Res*, 36(5):631–644.
- 18 Lee, B. B., Kremers, J., and Yeh, T. (1998). Receptive fields of primate retinal ganglion cells studied with a novel technique. *Vis Neurosci*, 15:161–175.
- 21 Lee, B. B., Pokorny, J., Smith, V. C., Martin, P. R., and Valberg, A. (1990). Luminance and chromatic modulation sensitivity of macaque ganglion cells and human observers. *J Opt Soc Am A*, 7(12):2223–2236.
- 25 Lee, B. B., Wehrhahn, C., Westheimer, G., and Kremers, J. (1993). Macaque ganglion cell responses to stimuli that elicit hyperacuity in man: detection of small displacements. *J Neurosci*, 13:1001–1009.
- 29 Leventhal, A. G., Rodieck, R. W., and Dreher, B. (1981). Retinal ganglion cell classes in the Old World monkey: morphology and central projections. *Science*, 213(4512):1139–1142.
- 33 Martinez-Conde, S., Macknik, S., and Hubel, D. (2004). The role of fixational eye movements in visual perception. *Nat Rev Neurosci*, 5(3):229–240.
- 36 Masu, M., Iwakabe, H., Tagawa, Y., Miyoshi, T., Yamashita, M., Fukuda, Y., Sasaki, H., Hiroi, K., Nakamura, Y., and Shigemoto, R. (1995). Specific deficit of the ON response in visual transmission by targeted disruption of the mGluR6 gene. *Cell*, 80(5):757–765.
- 40 Mather, G. (2000). Integration biases in the Ouchi and other visual illusions. *Perception*, 29(6):721–727.
- 44 McMahan, M. J., Packer, O. S., and Dacey, D. M. (2004). The classical receptive field surround of primate parasol ganglion cells is mediated primarily by a non-GABAergic pathway. *J Neurosci*, 24(15):3736–3745.
- 47 Merigan, W. H. and Maunsell, J. H. (1993). How parallel are the primate visual pathways? *Annu Rev Neurosci*, 16:369–402.
- 50 Milam, A. H., Dacey, D. M., and Dizhoor, A. M. (1993). Recoverin immunoreactivity in mammalian cone bipolar cells. *Vis Neurosci*, 10(1):1–12.
- 53 Murakami, I. (2004). Correlations between fixation stability and visual motion sensitivity. *Vision Res*, 44(8):751–761.

- 1
2
3
4
5
6
7
8
9 Murakami, I., Kitaoka, A., and Ashida, H. (2006). A positive correlation between fixation instability and the strength of illusory motion in a static display. *Vision Res*, 46(15):2421–2431.
- 10
11
12 Nirenberg, S. and Meister, M. (1997). The light response of retinal ganglion cells is truncated by a displaced amacrine circuit. *Neuron*, 18:637–650.
- 13
14
15 O’Brien, B. J., Richardson, R. C., and Berson, D. M. (2003). Inhibitory network properties shaping the light evoked responses of cat alpha retinal ganglion cells. *Vis Neurosci*, 20(4):351–361.
- 16
17
18
19 Pack, C. C. and Born, R. T. (2001). Temporal dynamics of a neural solution to the aperture problem in visual area MT of macaque brain. *Nature*, 409(6823):1040–1042.
- 20
21
22 Pirenne, M. H., Compbell, F. W., Robson, J. G., and MacKay, D. M. (1958). Moving visual images produced by regular stationary patterns. *Nature*, 181(4605):362–363.
- 23
24
25
26 Riggs, L. A. and Ratliff, F. (1951). Visual acuity and the normal tremor of the eyes. *Science*, 114(2949):17–18.
- 27
28
29 Roska, B., Nemeth, E., and Werblin, F. S. (1998). Response to change is facilitated by a three-neuron disinhibitory pathway in the tiger salamander. *J Neurosci*, 18(9):3451–3459.
- 30
31
32
33 Schiller, P. H. and Logothetis, N. K. (1990). The color-opponent and broad-band channels of the primate visual system. *Trends Neurosci*, 13(10):392–398.
- 34
35
36 Schnapf, J. L., Nunn, B. J., Meister, M., and Baylor, D. A. (1990). Visual transduction in cones of the monkey macaca fascicularis. *J Physiol*, 427:681–713.
- 37
38
39
40 Sinclair, J. R., Jacobs, A. L., and Nirenberg, S. (2004). Selective ablation of a class of amacrine cells alters spatial processing in the retina. *J Neurosci*, 24(6):1459–1467.
- 41
42
43 Spauschus, A., Marsden, J., Halliday, D. M., Rosenberg, J. R., and Brown, P. (1999). The origin of ocular microtremor in man. *Exp Brain Res*, 126.
- 44
45
46
47 Steinman, R. M., Cunitz, R. J., Timberlake, G., and Herman, M. (1967). Voluntary control of microsaccades during maintained monocular fixation. *Science*, 155:1577–1579.
- 48
49
50
51 Steinman, R. M., Haddad, G. M., Skavenski, A. A., and Wyman, D. (1973). Miniature eye movement. *Science*, 181(102):810–819.
- 52
53
54 Vardi, N., Zhang, L.-L., Payne, J. A., and Sterling, P. (2000). Evidence that different cation chloride cotransporters in retinal neurons allow opposite responses to GABA. *J Neurosci*, 20(20):7657–7663.
- 55
56
57
58
59
60
61
62
63
64
65

- 1
2
3
4
5
6
7
8
9 Victor, J. D. (1988). The dynamics of cat retinal Y cell subunit. *J Physiol*,
10 405:289–320.
11
12 Wade, N. J. (2003). Movements in art: from Rosso to Riley. *Perception*,
13 32(9):1029–1036. *Biography*.
14
15 Wallach, H. (1935). Über visuell wahrgenommene Bewegungsrichtung. *Psychol*
16 *Forsch*, 20:325–380.
17
18 Wässle, H. and Boycott, B. B. (1991). Functional architecture of the mammalian
19 retina. *Physiol Rev*, 71(2):447–479.
20
21 Wässle, H., Boycott, B. B., and Röhrenbeck, J. (1989). Horizontal cells in the
22 monkey retina: cone connections and dendritic network. *Eur J Neurosci*,
23 1:421–435.
24
25 Westheimer, G. (1986). *Handbook of Perception and Human Performance*,
26 volume 1, chapter The eye as an optical instrument. John Wiley & Sons,
27 New York.
28
29 White, A. J., Sun, H., Swanson, W. H., and Lee, B. B. (2002). An examination of
30 physiological mechanisms underlying the frequency-doubling illusion. *Invest*
31 *Ophthalmol Vis Sci*, 43(11):3590–3599.
32
33 Zanker, J. M. (2004). Looking at Op Art from a computational viewpoint. *Spat*
34 *Vis*, 17(1-2):75–94.
35
36 Zanker, J. M. and Walker, R. (2004). A new look at Op art: towards a simple
37 explanation of illusory motion. *Naturwissenschaften*, 91(4):149–156.
38
39
40
41
42
43
44
45
46
47
48
49
50
51
52
53
54
55
56
57
58

1
2
3
4
5
6
7
8
9
10
11
12
13
14
15
16
17
18
19
20
21
22
23
24
25
26
27
28
29
30
31
32
33
34
35
36
37
38
39
40
41
42
43
44
45
46
47
48
49
50
51
52
53
54
55
56
57
58
59
60
61
62
63
64
65

Figure 1: Structure of the Model. A, Schematic circuit diagram of the model retina. Photoreceptors (P) connect by excitatory synapses (\oplus) to horizontal cells (H) and by sign-inverting synapses (\ominus) to On-centre bipolar cells (BC). Horizontal cells connect to bipolar cells with sign-conserving synapses. The receptive field of On-centre ganglion cells (GC) consists of excitatory input from On-centre bipolar cells (centre) and inhibitory input from wide field amacrine cells (A, surround). For MC-cells, the presynaptic bipolar cells receive inhibition from narrow-field amacrine cells (N) at the axon terminal (thereby forming a subgroup of transient bipolar cells). Narrow field amacrine cells receive excitatory input from bipolar cells and inhibition from wide field amacrine cells (W). Wide field amacrine cells are excited by transient bipolar cells and receive inhibition from narrow-field amacrine cells. Combined, this coupling of amacrine cells forms a nested circuit (shaded region), which leads to transient responses in MC-ganglion cells. B, Spatial parameters of the simulated network (relative sizes are to scale). Shown are the point spread function simulating ocular blurring, the separation of photoreceptors (open circles), and PC- and MC-ganglion cells (filled circles). C, Responses of a photoreceptor, sustained and transient bipolar cell and PC- and MC-ganglion cell during contrast reversal of a sinusoidal grating (at the 90 deg phase, 11 cpd, 5Hz).

Figure 2: Simulated fixational eye movements. A, Power spectrum of the simulated fixational eye movements. B, Example trace of simulated eye movements. The inset shows 2s of slow drift movements as recorded by Murakami (2004) (vertical calibration bar indicates 20'). C, Velocity distributions of the slow drift movements. The velocities were obtained after resampling the eye movement traces at 1kHz, to allow for comparison with experimental data.

Figure 3: Population activity of retinal ganglion cells during presentation of a star-shaped stimulus (at half-saturating photoreceptor luminance, 100% contrast, diameter 110', bar width 2.86') A, Schematic drawing of the stimulus. Bars indicate where the single cell activity in panels G (red) and H (blue) was recorded. B, Simulated horizontal (red) and vertical (blue) eye movements. t_1 and t_2 indicate where the snapshots in C,D and E,F were taken. The relative 2-dimensional motion direction is indicated by arrows. C-F, Spatial population activity of PC-cells (C and D) and MC-cells (E and F), taken at t_1 and t_2 , as indicated in B. G, Activity of single photoreceptors, PC- and MC-cells at a location where axial fading is visible at time t_2 (red bar in A). The asterisks indicates where fading occurs in PC- and MC-cells (the location marked by an asterisk in A). H, as (G), but illustrating line splitting. Responses were taken from the region marked by a blue bar in A. Diamonds indicate where splitting is visible. In G and H, ganglion cell responses were clipped below resting potential to enhance visibility of the effects. Calibration bars correspond to 3 mV membrane potential.

1
2
3
4
5
6
7
8
9
10
11
12
13
14
15
16
17
18
19
20
21
22
23
24
25
26
27
28
29
30
31
32
33
34
35
36
37
38
39
40
41
42
43
44
45
46
47
48
49
50
51
52
53
54
55
56
57
58
59
60
61
62
63
64
65

Figure 4: Nonlinear spatial summation in MC-cells causes the splitting percept. A, Simulated responses (150ms) of photoreceptors; B, their temporal derivatives calculated numerically and C, MC-cell responses to two lines of the star-shaped stimulus calculated with the full model. Brackets indicate the central $7'$ of the MC-cell receptive field. The response of the differentiated signals (B) summed across the bracket after inversion are shown in D (upper trace: raw data, lower trace: after low-pass filtering with $\tau = 4ms$). The low-pass filtered trace is also shown in C. All responses were taken from the simulations shown in Figure 3. Calibration bars indicate 5 mV.

Figure 5: Effect of modifications of the model on the line-splitting effect. Each panel shows a snapshot of the ganglion cell population response during stimulation with the star-shaped stimulus (Fig. 3A, at saturating photoreceptor luminance, 100% contrast, diameter $91'$, bar width $2.4''$). A, B, responses for the full PC- and MC-cell model, respectively. The circle in B indicates a location where line-splitting occurs. C, MC-cell responses after replacing the original photoreceptor model with a linear model. D, MC-cell response with an inactivated nested amacrine circuit. E, Response for MC-cells, when the receptive field centre consists of a single cone.

Figure 6: Supporting online material - movies: The two movies show the spatiotemporal activity of a grid of simulated PC- and MC-cells (diameter $110'$) during stimulation with the star shaped stimulus (450 ms stimulus duration). The relative stimulus position is shown at the top of each frame (blue: horizontal displacement, green: vertical displacement). Below, the membrane potential of the ganglion cells is color coded for each neuron. The movies illustrate the main findings of the model study: (1) A substantial axial fading occurs in MC-cells and, much weaker, in PC-cells. It is visible along various directions, which are directly related to the motion of the stimulus on the retina. (2) Line-splitting, as described in this work, can be seen as additional yellow and red lines in the MC-cell population response, but not in that of PC-cells.

1
2
3
4
5
6
7
8
9
10
11
12
13
14
15
16
17
18
19
20
21
22
23
24
25
26
27
28
29
30
31
32
33
34
35
36
37
38
39
40
41
42
43
44
45
46
47
48
49
50
51
52
53
54
55
56
57
58
59
60
61
62
63
64
65

Parameter	Eqns.	Description	Value
$S_i(t)$	3	Activity of the i-th low-pass filter stage (i=1..3, i=0: Stimulus). Emulates the initial amplification cascade.	
τ_{Casc}	3	Time constant of the low-pass filter.	$2ms$
$[cGMP](t)$	4	Concentration of hydrolyzed cGMP.	
β	4	Strength of the re-synthesis reaction of cGMP.	$1ms^{-1}$
$[Ca^{2+}](t)$	5	Intracellular concentration of Ca^{2+} .	
α, γ	5	Rates of efflux and influx of ions.	$0.4ms^{-1}$
c	5	Impact of $[cGMP]$ on the cation concentration.	$0.1ms^{-1}$
$[H](t)$	6	Hyperpolarization-activated I_h current.	
$V_P(t)$	7	Photovoltage.	
A_H	6	Activation of the h-current.	$-0.4V$
S_H	6	Slope of the activation function for the h-current.	$10V^{-1}$
δ_H	6	Rates of increase and decay of the ionic concentrations for the h-current.	$0.025ms^{-1}$
C_P	7	Membrane capacity.	$100pF$
q_P	7	Unit charge transported by the Ca^{2+} current.	$1 \cdot 10^{-9}C$
q_I	7	Unit charge transported by the I_h current.	$6 \cdot 10^{-9}C$

Table 1: Constants, variables and parameters of the photoreceptor model. It consists of the following stages: (1) three cascaded low-pass filters (Eqn. 3), (2) hydrolysis of the second messenger cGMP (Eqn. 4) and Ca^{2+} -dependent re-synthesis, (3) in- and outflux of Ca^{2+} (Eqn. 5), (4) the hyperpolarization-activated I_h current (Bader and Bertrand, 1984; Demontis et al., 1999) (Eqn. 6) and the calculation of the photovoltage (Eqn. 7). Concentrations of second messengers and cations are calculated in dimensionless units relative to the boundaries $[0, 1]$ and the photovoltage is calculated in Volts.

Figure 1
[Click here to download Figure: Fig1.eps](#)

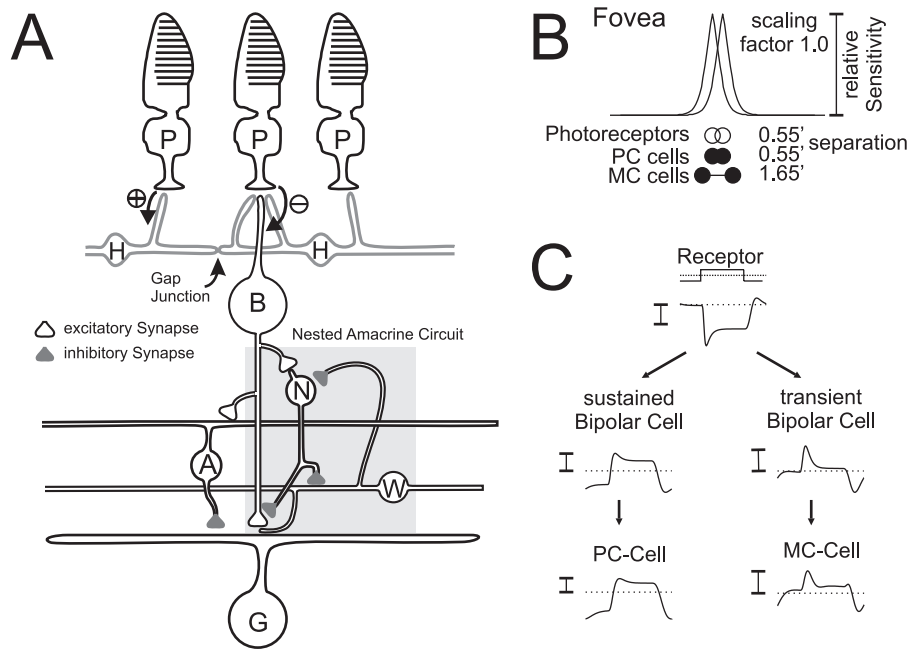


Figure 2
[Click here to download Figure: Fig2.eps](#)

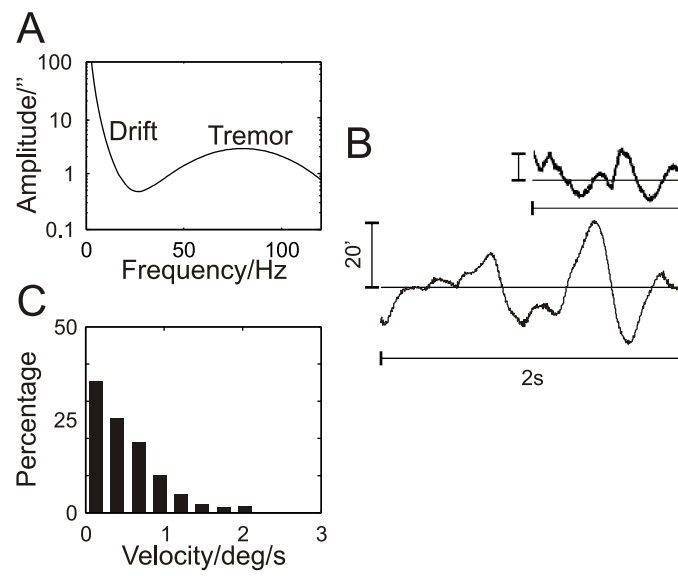


Figure 3
[Click here to download Figure: Fig3.eps](#)

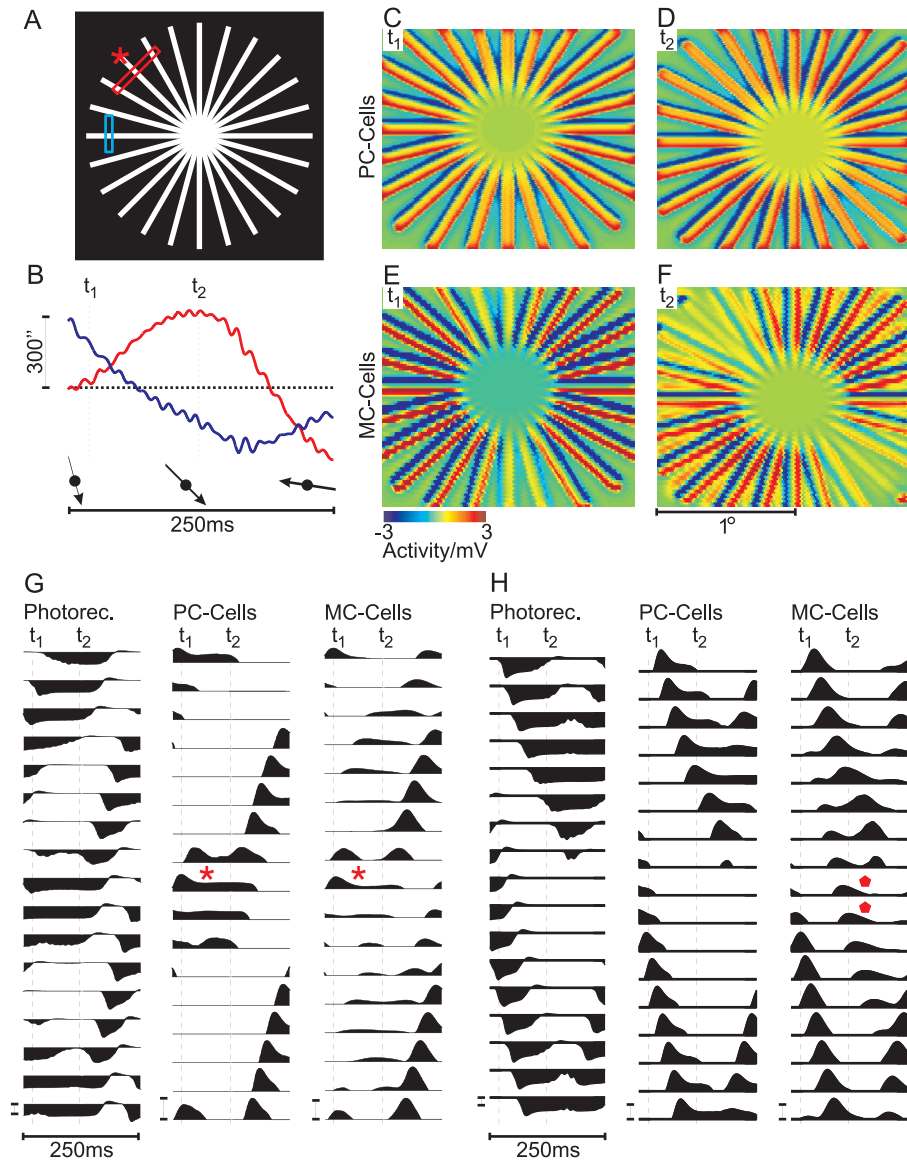


Figure 4
[Click here to download Figure: Fig4.eps](#)

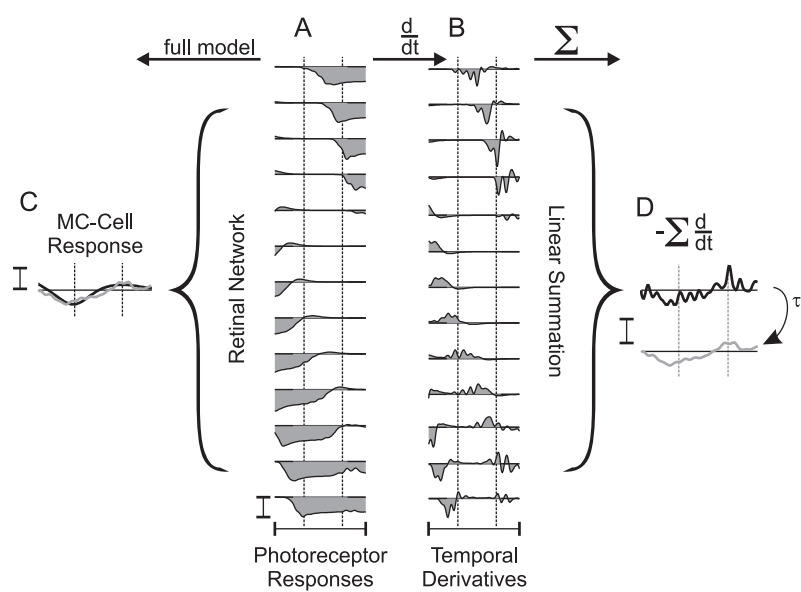


Figure 5
[Click here to download Figure: Fig5.eps](#)

